Institut Riset dan Publikasi Indonesia (IRPI)
MALCOM: Indonesian Journal of Machine Learning and Computer Science
Journal Homepage: https://journal.irpi.or.id/index.php/malcom
Vol. 5 Iss. 1 January 2025, pp: 258-264
ISSN(P): 2797-2313 | ISSN(E): 2775-8575

Three-Phase Space Vector Pulse Width Modulation with Proportional Integral Derivative Control for High-Capacity Battery Charging

Elvin Nursandi[1*], Charles Ronald Harahap[2], Fx Arinto Setyawan[3]

[1,2,3]Department of Electrical Engineering, Faculty of Engineering,
Universitas Lampung, Indonesia

E-Mail: [1]elvinnursandi2211@gmail.com,
[2]charles.harahap69@gmail.com, [3]fx.arinto@eng.unila.ac.id

Received Oct 10th 2024; Revised Dec 07th 2024; Accepted Dec 26th 2024; Available Online Dec 26th 2024; Published Jan 8th 2025
Corresponding Author: Elvin Nursandi

Abstract

The growing consumption electricity has burdened the existing power grid, potentially leading to overloads and power outages when supply does not meet demand. Integrating alternative resources, such as Gas Power Plants (PLTG), as backup solutions can mitigate these risks. PLTG relies on various DC components to power the machines, all supplied by a high-capacity battery bank. This research is conducted at the PLTG UPK Sebalang, where the existing system cannot stabilize the rectifier voltage during battery charging. As a result, failures occur during the generator starting process. Therefore, this study aims to stabilize the output voltage of the existing three-phase rectifier system at PLTG UPK Sebalang. To achieve this goal, the Space Vector Pulse Width Modulation (SVPWM) rectifier with Proportional Integral Derivative (PID) control method is proposed. This method dynamically reduces steady-state error to produce a stable output voltage from the rectifier. In repetitive experiments, the system effectively kept the rectifier voltage stable at 125V, experiencing an average decrease of just 1.05%.

Keywords: Battery Charging Control, PID Control, PLTG UPK Sebalang, SVPWM Rectifier

1. INTRODUCTION

The increasing demand for electricity has caused an overload in the grid. This occurs when electricity demand surpasses supply, potentially leading to system failure and blackouts in the transmission network [1], [2]. A solution to this issue is to integrate alternative power plants, such as gas power plants, as a backup supply.

During a blackout, most power generation units cannot operate normally, which impacts the electricity generation capacity of the transmission system, making it much lower than the load demand and potentially leading to transmission network outages. When this occurs, the electric power system must quickly normalize the transmission network to resume serving the load or electricity users. In relation to this condition, the Sebalang Power Generation Unit (UPK Sebalang) has a gas power plant (PLTG) that acts as a power transfer unit during a blackout. This plant is connected to the 150KV transmission network and is referred to as a black start generator.

However, in reality, the PLTG cannot operate if the direct current (DC) system of the battery does not function optimally. The most common failure in a power plant that uses an engine is battery failure, accounting for at least 30% of total failures [3,4]. Therefore, battery replacement in the PLTG is necessary. To address this issue, a stable rectifier is needed to charge the high-capacity batteries used in the PLTG.

Recently, several studies have addressed this issue. Mansouri et al. [5] introduced a three-phase Space Vector Pulse Width Modulation (SVPWM) rectifier that utilizes the Artificial Neural Network (ANN) approach to maintain a stable voltage for renewable energy storage. Ali et al. [6] developed a three-level T-type Vienna rectifier employing a soft-switching technique. Teng et al. [7] proposed a new SVPWM-based method for charging a 48V battery. These studies demonstrate encouraging results with low power loss, though complexity remains a challenge to be addressed.

Fuzzy control is a modern approach that combines automatic control technology with Fuzzy system theory, making it highly effective for managing the challenges of non-linear systems [8]. Some studies use a Fuzzy Logic Controller to enhance rectifier performance [9,10], generating a PWM signal based on power from renewable energy sources. This approach enables an adaptive response with minimal circuit

modifications. However, it slows down the response system. This limitation can be addressed by using a more straightforward controller, such as a PID controller [11,12].

In this paper, we propose a three-phase SVPWM rectifier designed to generate a constant voltage for effective battery charging. Recognizing the limitations identified in previous studies, we introduce a PID control method aimed at enhancing the response of the existing rectifier system. This method leverages the principles of proportional, integral, and derivative control to provide more accurate voltage regulation and improved dynamic performance.

2. MATERIALS AND METHOD

This section describes the mathematical modeling of the three-phase SVPWM rectifier presented in this study. It includes SVPWM vector control and proposed PID control. While this study highlights the application for rectifiers, it can similarly be applied to three-phase SVPWM inverter applications [13,18].

2.1. The Direct Quadrature Voltage Vector

The dq-axes are made up of the d-axis and the q-axis within a $dq0$-coordinate system. The voltage on the d-axis corresponds to a three-phase source represented in direct current form, while the voltage on the q-axis is zero [19]. O'Rourke et al. [20] analyze the Clarke and Park transformations, which involve quantities such as abc, $\alpha\beta 0$, and $dq0$. The voltage transformation from abc to $dq0$ is illustrated in Equations (1), (2), and (3).

$$\left[V_\alpha\ V_\beta\ V_0\ \right] = \frac{2}{3}\begin{bmatrix} 1 & -\frac{1}{2} & -\frac{1}{2} \\ 0 & \sqrt{\frac{3}{2}} & -\sqrt{\frac{3}{2}} \\ \frac{1}{2} & \frac{1}{2} & \frac{1}{2} \end{bmatrix} [V_{a1}\ V_{b1}\ V_{c1}\ ] \tag{1}$$

$$\left[V_\alpha\ V_\beta\ V_0\ \right] = \begin{bmatrix} \frac{2}{3} & -\frac{1}{3} & -\frac{1}{3} \\ 0 & \frac{1}{\sqrt{3}} & -\frac{1}{\sqrt{3}} \\ \frac{1}{3} & \frac{1}{3} & \frac{1}{3} \end{bmatrix} [V_{a1}\ V_{b1}\ V_{c1}\ ] \tag{2}$$

$$\left[V_d\ V_q\ V_0\ \right] = [cos\ cos\ (\theta t)\ \ sin\ sin\ (\theta t)\ \ 0\ (\theta t)\ \ cos\ cos\ (\theta t)\ \ 0\ 0\ 0\ 1\ ]\left[V_\alpha\ V_\beta\ V_0\ \right] \tag{3}$$

2.2. SVPWM Vector Control

The proposed system puts forward SVPWM conventional configuration as shown in Table 1. Figure 1 illustrates each sector, with each sector covering a 60° angle. In this configuration, V_0 and V_7 represent zero vectors, while V_1 through V_6 are nonzero space vectors. The angle θ rotates anticlockwise from 0° to 360° along the axis, specifically revolving from 0° to 60° between two axes. Each sector contains two space vectors that correspond to the switching configurations of the transistors, enabling efficient operation of the rectifier system. This approach ensures effective control of the voltage output in the three-phase SVPWM rectifier.

Table 1. Switching Sequences of SVPWM

Sector	Switching Sequence
1	$V_0, V_1, V_2, V_7, V_2, V_1, V_0$
2	$V_0, V_3, V_2, V_7, V_2, V_3, V_0$
3	$V_0, V_3, V_4, V_7, V_4, V_3, V_0$
4	$V_0, V_5, V_4, V_7, V_4, V_5, V_0$
5	$V_0, V_5, V_6, V_7, V_6, V_5, V_0$
6	$V_0, V_1, V_6, V_7, V_6, V_1, V_0$

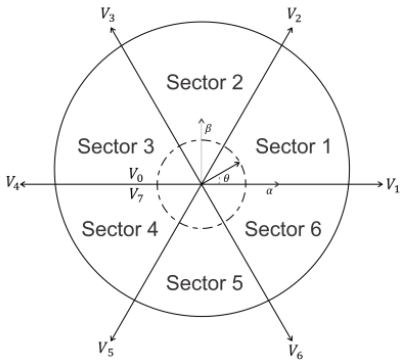

Figure 1. Voltage Space Vector Diagram

2.3. PID Control

Figure 2 illustrates a simplified block diagram of the SVPWM rectifier, with the proposed PID method. This approach aims to enhance the transient response, particularly in reaction to abrupt and fluctuating changes in the rectifier loads. As noted in the previous section, the output voltage of the rectifier is directly proportional to the load current, meaning that V_{dc} varies linearly with the battery's State of Charge (SOC). In light of this situation, the PID constants are then chosen accordingly. The Equations (4), (5), and (6) show the mathematical representation of gains P, I, and D respectively.

$$P = K_p e(t) \tag{4}$$

$$I = K_i \int_0^t e(\tau) d\tau \tag{5}$$

$$D = K_d \frac{de(t)}{dt} \tag{6}$$

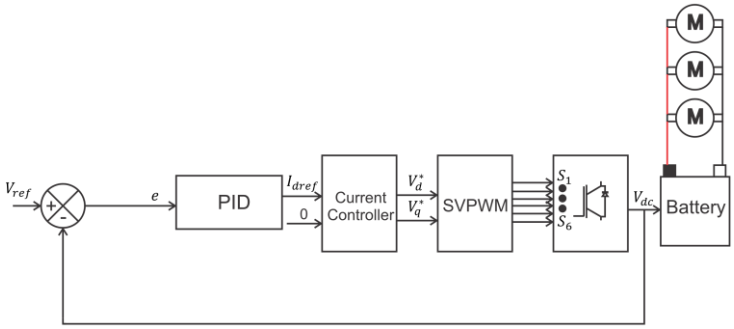

Figure 2. Block Diagram of Proposed PID Control

PID gains are determined based on experimental results; therefore, the rectifier's responses are observed while varying the State of Charge (SoC) from 0% to 100%. This comprehensive analysis allows us to assess how the rectifier behaves across the entire range of battery charge levels. By closely monitoring the system's performance under these conditions, we can identify the optimal PID parameters that ensure efficient operation and stable voltage regulation throughout the charging process.

3. RESULTS AND DISCUSSION

This section analyzes the experimental results of the proposed system. The findings are presented to assess the system's effectiveness in generating a constant voltage across various scenarios compared to an existing system. Following this, a comparison with the existing PI system as previously analyzed in the work conducted by [21] is conducted to evaluate the performance of the proposed system.

3.1. Experimental Setup

The experiment is conducted based on the parameters outlined in Table 2. Figure 3 illustrates the experimental setup for the proposed rectifier system. In this setup, the rectifier module is connected to a lithium battery bank and three motors, which are utilized to initiate the gas power plant generator. The primary focus of the experiment is to analyze the output of the rectifier when it is linked to the battery bank, particularly with the additional parallel connection of the three motors. This arrangement allows for a comprehensive evaluation of the rectifier's performance in real-world conditions, as it operates under the influence of both the battery and the motors.

Table 2. System Parameters

Parameter	Value
Grid Voltage (RMS): V_{abc} /V	380
Frequency: f/Hz	50
Inductor Filter: L_f/mH	0.5
Capacitor Filter: C_f/mF	0.1
DC bus Capacitor: C/mF	5.6
Battery Voltage: V_b/V	125
Battery Capacity: C_A/Ah	200
Motor Load: I_l/A	150.25

Parameter	Value
Proportional: P	2
Integral: I	500
Derivative: D	10

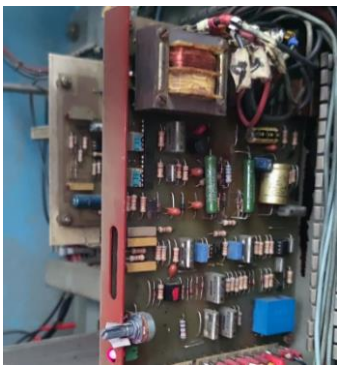

Figure 3. Experimental Setup of the Proposed System.

The $P, I,$ and D parameters represent proportional, integral, and derivative gains of the controller respectively. These parameters are tuned manually by considering the step response of a controller. Initially, P gain is selected at a minimum level to prevent excessive oscillation. Once the proportional gain is appropriately adjusted, I is introduced to address and eliminate steady-state error, ensuring the system reaches and maintains its desired setpoint over time. Following this, the D is applied to minimize the overshoot that may result from a high integral gain, thereby improving the system's responsiveness and reducing the oscillation.

3.2. SVPWM Signal Response

Figure 4 shows the SVPWM signal response sampled at a frequency of 10 kHz. From the figure, it can be observed that there are six SVPWM signals used to control each IGBT in the system. In this context, these signals are divided into two main groups.

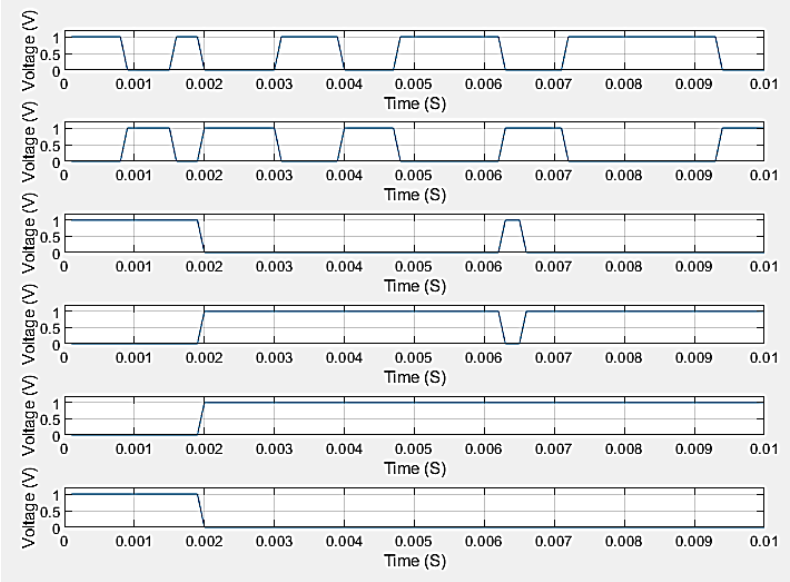

Figure 4. SVPWM Signal Response

Signals S_1, S_3, and S_5 are the primary signals that directly influence the output voltage of the rectifier. These signals are responsible for determining the ON duration of each IGBT, which in turn affects the magnitude and quality of the DC voltage produced by the rectifier.

In contrast, signals S_2, S_4, and S_6 are the inverse signals of the primary signals. These inverse signals are designed to provide balance within the system by ensuring that each IGBT operates in the appropriate sequence to effectively regulate the phase of the voltage and current. In other words, these inverse signals assist in maintaining the stability and efficiency of the power conversion process, reducing harmonic distortion, and ensuring more precise control over the output voltage.

3.3. Rectifier Step Response

A comparison is performed to evaluate the response as well as the performance of the proposed PID controller. In this scenario, the rectifier is tested while the battery is in charging mode with a motor load of 150.25 A. Figure 5 shows that the voltage of the rectifier in the existing PI system drops by 5.6% from the reference voltage. This decline is attributed to the lack of adaptive control, which results in a slower response from the rectifier. In contrast, the proposed rectifier system is able to maintain the voltage at the reference level. Although there is a voltage drop during the time frame of 0 to 0.2 seconds, the PID control successfully restores the voltage to a stable position within 1.78 seconds.

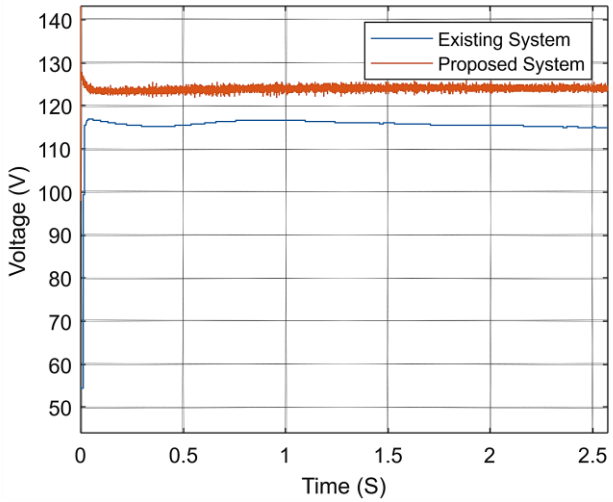

Figure 5. Step Response Comparison Between the Existing and Proposed Systems

3.4. Performance Analysis

In this section, tests are conducted on the current of the rectifier during the battery charging process. Figure 6 presents the charging current response from the point when the battery is empty until it is fully charged. Observations indicate that the proposed system successfully enhances the charging current by 55% compared to the existing system.

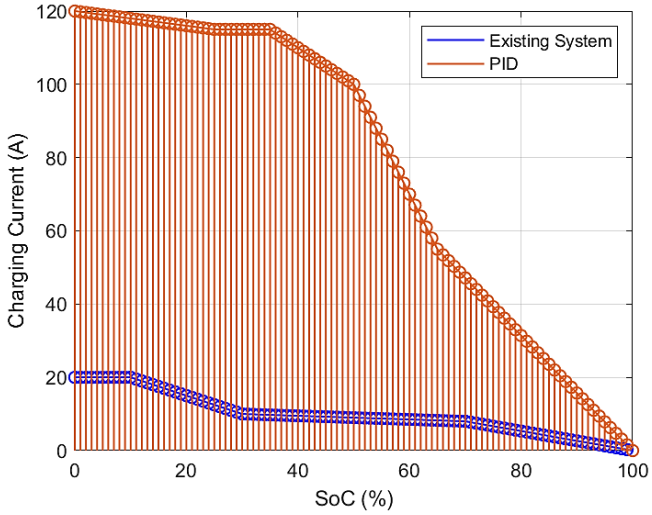

Figure 6. Battery Charging Current with the SoC of 0-100%

Considering a battery capacity of approximately 200 Ah, the proposed system can charge the battery from an empty state (0%) to a full in about 4.5 hours. This significant charging speed indicates that the proposed system provides much better efficiency compared to the existing model, as presented in Table 3. These findings highlight that the new system not only drastically improves the charging current but also accelerates the overall battery charging process.

Table 3. Comparison of Rectifier Performance

Existing System	Proposed System
The time to fully charge is about 10h	The time to fully charge is about 4.5h
Voltage drops gradually when motors are connected	Voltage stabilizes after 1.78s
Voltage drop is about 3.2%	Voltage drop is about 1.05%

4. CONCLUSION

Based on the design results and analysis of the experimental outcomes, it can be concluded that the proposed PID control-based rectifier system has proven effective in achieving stabilization of the rectifier voltage. In various experiments, the system successfully maintained the rectifier voltage at 125V, with an average drop of only 1.05%. Additionally, validation results indicate that the proposed PID method can replace the existing rectifier module in the UPK Sebalang gas power generation system. Notably, the proposed system is capable of charging 5.5 hours faster compared to the existing system, demonstrating its efficiency and effectiveness in enhancing overall performance. The proposed system still has limitations especially when handling non-linear loads. This problem can be addressed by incorporating sophisticated machine-learning algorithms into the controller. Such an enhancement has the potential to optimize the system's adaptability and performance in complex operating conditions.

REFERENCES

[1] H. Haes Alhelou, M. E. Hamedani-Golshan, T. C. Njenda, and P. Siano, "A Survey on Power System Blackout and Cascading Events: Research Motivations and Challenges," *Energies (Basel)*, vol. 12, no. 4, p. 682, Feb. 2019, doi: 10.3390/en12040682.

[2] J. Marqusee and D. Jenket, "Reliability of emergency and standby diesel generators: Impact on energy resiliency solutions," *Appl Energy*, vol. 268, p. 114918, Jun. 2020, doi: 10.1016/j.apenergy.2020.114918.

[3] P. Y. Du, J. Burnett, and S. M. Chan, "Reliability of standby generators in Hong Kong buildings," *IEEE Trans Ind Appl*, vol. 39, no. 6, pp. 1592–1595, Nov. 2003, doi: 10.1109/TIA.2003.818978.

[4] A. D'Orazio, S. Elia, E. Santini, and M. Tobia, "Succor System and Failure Indication for the Starter Batteries of Emergency Gensets," *Periodica Polytechnica Electrical Engineering and Computer Science*, vol. 64, no. 4, pp. 412–421, Sep. 2020, doi: 10.3311/PPee.15274.

[5] A. Mansouri, A. El Magri, R. Lajouad, and F. Giri, "Control design and multimode power management of WECS connected to HVDC transmission line through a Vienna rectifier," *International Journal of Electrical Power & Energy Systems*, vol. 155, p. 109563, Jan. 2024, doi: 10.1016/j.ijepes.2023.109563.

[6] A. Ali, J. Chuanwen, Z. Yan, S. Habib, and M. M. Khan, "An efficient soft-switched vienna rectifier topology for EV battery chargers," *Energy Reports*, vol. 7, pp. 5059–5073, Nov. 2021, doi: 10.1016/j.egyr.2021.08.105.

[7] H. Teng, Y. Zhong, and H. Bai, "SiC + Si three-phase 48 V electric vehicle battery charger employing current-SVPWM controlled SWISS AC/DC and variable-DC-bus DC/DC converters," *IET Electrical Systems in Transportation*, vol. 8, no. 4, pp. 231–239, Dec. 2018, doi: 10.1049/iet-est.2017.0083.

[8] X. Ge, F. W. Ahmed, A. Rezvani, N. Aljojo, S. Samad, and L. K. Foong, "Implementation of a novel hybrid BAT-Fuzzy controller based MPPT for grid-connected PV-battery system," *Control Eng Pract*, vol. 98, p. 104380, May 2020, doi: 10.1016/j.conengprac.2020.104380.

[9] T. Wang, C. Lin, K. Zheng, W. Zhao, and X. Wang, "Research on Grid-Connected Control Strategy of Photovoltaic (PV) Energy Storage Based on Constant Power Operation," *Energies (Basel)*, vol. 16, no. 24, p. 8056, Dec. 2023, doi: 10.3390/en16248056.

[10] S. Dadfar, K. Wakil, M. Khaksar, A. Rezvani, M. R. Miveh, and M. Gandomkar, "Enhanced control strategies for a hybrid battery/photovoltaic system using FGS-PID in grid-connected mode," *Int J Hydrogen Energy*, vol. 44, no. 29, pp. 14642–14660, Jun. 2019, doi: 10.1016/j.ijhydene.2019.04.174.

[11] Z. Shutuan, J. Jing, and Z. Kai, "A Novel Three-phase Rectifier Based on Improved PID Control Algorithm," *TELKOMNIKA Indonesian Journal of Electrical Engineering*, vol. 11, no. 1, Jan. 2013, doi: 10.11591/telkomnika.v11i1.1910.

[12] Z. Yao, "Analysis of Control Strategy of Three-phase Bridge Fully Controlled Rectifier Circuit Based on PID Control," *Highlights in Science, Engineering and Technology*, vol. 17, pp. 328–335, Nov. 2022, doi: 10.54097/hset.v17i.2623.

[13] J. Zheng, C. Peng, K. Zhao, and M. Lyu, "A Low Common-Mode SVPWM for Two-Level Three-Phase Voltage Source Inverters," *Energies (Basel)*, vol. 16, no. 21, p. 7294, Oct. 2023, doi: 10.3390/en16217294.

[14] H.-C. Cheng, Y.-C. Liu, H.-H. Lin, S.-C. Chiou, C.-M. Tzeng, and T.-C. Chang, "Development and Performance Evaluation of Integrated Hybrid Power Module for Three-Phase Servo Motor Applications," *Micromachines (Basel)*, vol. 14, no. 7, p. 1356, Jun. 2023, doi: 10.3390/mi14071356.

[15] J. Kim, M.-H. Nguyen, S. Kwak, and S. Choi, "Lifetime Extension Method for Three-Phase Voltage Source Converters Using Discontinuous PWM Scheme with Hybrid Offset Voltage," *Machines*, vol. 11, no. 6, p. 612, Jun. 2023, doi: 10.3390/machines11060612.

[16] R. Durgam, R. Karampuri, S. S. Rangarajan, U. Subramaniam, E. R. Collins, and T. Senjyu, "Investigations on the Modulation Strategies for Performance Improvement of a Controlled Wind Energy System," *Electronics (Basel)*, vol. 11, no. 23, p. 3931, Nov. 2022, doi: 10.3390/electronics11233931.

[17] R. Gong, H. Wu, J. Tang, and X. Wan, "A Modified SVPWM Strategy for Reducing PWM Voltage Noise and Balancing Neutral Point Potential," *Electronics (Basel)*, vol. 13, no. 9, p. 1656, Apr. 2024, doi: 10.3390/electronics13091656.

[18] N. Dinh Tuyen and L. Minh Phuong, "SVPWM Method for Multilevel Indirect Matrix Converter with Eliminate Common Mode Voltage," *Applied Sciences*, vol. 9, no. 7, p. 1342, Mar. 2019, doi: 10.3390/app9071342.

[19] I. Andrade, R. Pena, R. Blasco-Gimenez, J. Riedemann, W. Jara, and C. Pesce, "An Active/Reactive Power Control Strategy for Renewable Generation Systems," *Electronics (Basel)*, vol. 10, no. 9, p. 1061, Apr. 2021, doi: 10.3390/electronics10091061.

[20] C. J. O'Rourke, M. M. Qasim, M. R. Overlin, and J. L. Kirtley, "A Geometric Interpretation of Reference Frames and Transformations: dq0, Clarke, and Park," *IEEE Transactions on Energy Conversion*, vol. 34, no. 4, pp. 2070–2083, Dec. 2019, doi: 10.1109/TEC.2019.2941175.

[21] H. Teng, Y. Zhong, and H. Bai, "SiC + Si three-phase 48 V electric vehicle battery charger employing current-SVPWM controlled SWISS AC/DC and variable-DC-bus DC/DC converters," *IET Electrical Systems in Transportation*, vol. 8, no. 4, pp. 231–239, Dec. 2018, doi: 10.1049/iet-est.2017.0083.